Deoxycholate induced tetramer of αA-crystallin and sites of phosphorylation: Fluorescence correlation spectroscopy and femtosecond solvation dynamics

Aritra Chowdhury, Supratik Sen Mojumdar, Aparajita Choudhury, Rajat Banerjee, Kali Pada Das, Dibyendu Kumar Sasmal, and Kankan Bhattacharyya

Citation: The Journal of Chemical Physics **136**, 155101 (2012); doi: 10.1063/1.3702810
View online: http://dx.doi.org/10.1063/1.3702810
View Table of Contents: http://scitation.aip.org/content/aip/journal/jcp/136/15?ver=pdfcov
Published by the AIP Publishing

Deoxycholate induced tetramer of αA-crystallin and sites of phosphorylation: Fluorescence correlation spectroscopy and femtosecond solvation dynamics

Aritra Chowdhury,[1,a)] Supratik Sen Mojumdar,[2] Aparajita Choudhury,[1] Rajat Banerjee,[1,b)] Kali Pada Das,[3,b)] Dibyendu Kumar Sasmal,[2] and Kankan Bhattacharyya[2,b)]
[1]*Dr. B. C. Guha Centre for Genetic Engineering and Biotechnology and Department of Biotechnology, University of Calcutta, Ballygunge Circular Road, Kolkata-700019, India*
[2]*Department of Physical Chemistry, Indian Association for the Cultivation of Science, Jadavpur, Kolkata-700032, India*
[3]*Department of Chemistry, Bose Institute, 93/1 A.P.C. Road, Kolkata-700 009, India*

(Received 31 January 2012; accepted 27 March 2012; published online 16 April 2012; publisher error corrected 18 April 2012)

Structure and dynamics of acrylodan labeled αA-crystallin tetramer formed in the presence of a bile salt (sodium deoxycholate, NaDC) has been studied using fluorescence correlation spectroscopy (FCS) and femtosecond up-conversion techniques. Using FCS it is shown that, the diffusion constant (D_t) of the αA-crystallin oligomer (mass ~800 kDa) increases from ~35 μm^2 s^{-1} to ~68 μm^2 s^{-1}. This corresponds to a decrease in hydrodynamic radius (r_h) from ~6.9 nm to ~3.3 nm. This corresponds to about 10-fold decrease in molecular mass to ~80 kDa and suggests formation of a tetramer (since mass of αA-crystallin monomer is ~20 kDa). The steady state emission maximum and average solvation time ($\langle\tau_s\rangle$) of acrylodan labeled at cysteine 131 position of αA-crystallin is markedly affected on addition of NaDC, while the tryptophan (trp-9) becomes more exposed. This suggests that NaDC binds near the cys-131 and makes the terminal region of αA-crystallin exposed. This may explain the enhanced auto-phosphorylation activity of αA-crystallin near the terminus of the 173 amino acid protein (e.g., at the threonine 13, serine 45, or serine 169 and 172) and suggests that phosphorylation at ser-122 (close to cys-131) is relatively less important. © *2012 American Institute of Physics*. [http://dx.doi.org/10.1063/1.3702810]

I. INTRODUCTION

α-crystallin is a small heat shock protein (sHSP) and is a major constituent of the mammalian eye lenses.[1,2] It consists of two highly homologous chains αA- and αB- chains, containing, respectively, 173 and 175 amino acids with a molecular mass ~20 kDa.[3–7] In the eye lens αA- and αB-crystallins (in a molar ratio of ~3:1) are present as a large oligomeric complex of molecular mass ~800 kDa.[4] The recombinant αA-crystallin also exhibits similar oligomerization leading to a large size (300–1000 kDa).[8] α-crystallin has been demonstrated to be an efficient molecular chaperone that can recognize early unfolding intermediates and prevent aggregation of other proteins.[9–16] The chaperone function of α-crystallin is crucial in maintaining transparency and integrity of the eye lens.

Unlike other sHSP members quaternary-structural heterogeneity is idiosyncratic of α-crystallin and one of the likely causes for failures to crystallize it.[17,18] Although there is no strict correlation between oligomeric size and chaperone activity,[19] existing literature suggests that oligomerization is prerequisite for its chaperone like function.[5] The oligomer is dynamic in nature and subunits can exchange between different oligomers.[20,21] Various structural models were proposed to explain the oligomeric association of α-crystallin.[22–25] Experimental study of the smallest unit of α-crystallin is very few. A recombinant preparation of a truncated αB-crystallin (αB57-157) containing only the central "αA-crystallin domain" assembled in solution as a dimer and showed chaperone activity.[26] Merck *et al.* reported that C-terminal domain of α-crystallin formed dimers or tetramers.[27] Very recently a solid state NMR and small-angle x-ray scattering (SAXS) study proposed a dimeric unit of αB-crystallin as the building block.[28]

On addition of various surfactants the oligomer of α-crystallin continuously decreases in size on increasing the concentration of the amphiphilic molecules.[29–31] Using gel filtration chromatography Kantorow *et al.* demonstrated that addition of 1 wt. % sodium deoxycholate (NaDC) causes disaggregation of the α-crystallin aggregates (~800 kDa) to form a tetrameric species of mass ~80 kDa.[29] The reduction in size is accompanied by a 10-fold increase in auto-phosphorylation (Scheme 1(a)) activity of the tetrameric αA-crystallin.[29] NaDC does not increase auto-phosphorylation activity of αB-crystallin.[29] This result underlines the functional differences between αA- and αB-crystallin.

αA-crystallin has been reported to have autophosphorylation activity.[29,32,33] A number of researchers have confirmed the involvement of ser-122 as one of the most prominent sites of phosphorylation in the αA-crystallin

a)Present address: School of Chemistry, University of Manchester, Oxford Road, M13 9PL, Manchester, United Kingdom.
b)Authors to whom correspondence should be addressed: Electronic mail: pckb@iacs.res.in, rbbcgc@gmail.com, and kalipada@bosemain.bosinst.ac.in. Fax: (91)-33-2473-2805.

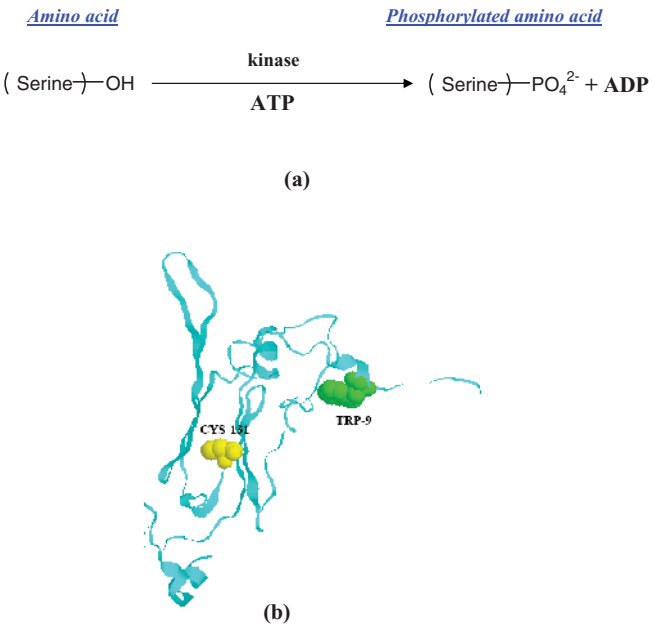

SCHEME 1. (a) Schematic representation of phosphorylation of amino acid. (b) Schematic structure of αA-crystallin subunit (obtained from I-Tasser web server[60,61]). Cystein is represented in yellow and tryptophan is in Green. The backbone structure of αA-crystallin subunit is represented as ribbon, while both the Cys and Trp residues are showed as spacefill display.

oligomer although other residues, such as thr-13 and 140, ser-45, 169, and 172, have also been reported as additional sites of phosphorylation.[29,32,33] On the contrary when αA-crystallin was converted into a tetramer in presence of NaDC, there is clearly no evidence for the involvement of ser-122 in the phosphorylation although there were 10-fold enhancements in autophosphorylation activity.[29] Reasons for the hyperphosphorylation and protection of ser-122 against phosphorylation of αA-crystallin in its tetrameric form still remain obscure. Besides the role of NaDC in the modulation of the autophosphorylation, properties of αA-crystallin as well as the exact binding site of NaDC to αA-crystallin have not been elucidated. In this work we attempt to throw new light on the site of binding of NaDC to αA-crystallin and on possible sites of phosphorylation in the NaDC induced tetramer of αA-crystallin.

To address this issue we employ fluorescence correlation spectroscopy (FCS), steady state, and femtosecond time resolved emission spectroscopy. First, using FCS we measure the size (hydrodynamic radius) of the αA-crystallin in the absence and presence of NaDC and show that addition of NaDC indeed leads to decrease in size. Second, from the position of emission maximum and quenching studies we show that NaDC causes crowding at around cys-131 in the αA-crystallin domain (Scheme 1(b)), while it makes the region near tryptophan (near N-terminus) more exposed. Third, we study solvation dynamics of the acrylodan covalently attached to cys-131. We show that solvation dynamics of the water molecules around this site becomes 2-fold slower on addition of NaDC. This conclusively shows that NaDC binds near cys-131 residue of αA-crystallin. This is very similar to the slowing down of the solvation dynamics at the active site of the enzyme on binding of a substrate, reported in our earlier works.[34]

It may be recalled that in recent years many groups have studied solvation dynamics of the biological water near protein using femtosecond time resolved fluorescence,[34–39] analytical theory,[40,41] and as computer simulation.[42–46] According to this studies biological water or water near a protein is several orders of magnitude slower than ordinary water in bulk.

II. MATERIALS AND METHODS

A. Materials

Spectra grade Acrylodan (6-acrylolyl-2-dimethylaminonaphtalene) (Scheme 2(a)) and 1,5-IAEDANS [5-((((2-iodoacetyl)amino)ethyl)amino) naphthalene-1-sulfonic acid] (Scheme 2(b)), purchased from Molecular Probes (USA), and used as received. Sephacryl S300-HR, sodium deoxycholate (NaDC), DTT (Dithiothreitol), IPTG (Isopropyl β-D-thiogalactoside), Urea, DNase, and lysozyme were obtained from Sigma (St. Louis, MO, USA).

B. Overexpression and purification of αA-crystallin

Recombinant αA-crystallin (Scheme 1(b)) was overexpressed and purified as mentioned before.[47] Briefly, αA-crystallin cDNA cloned in pAED4 vector was transformed in *E.coli* BL21-DE3 strain. Cultures grown in LB medium at 37 °C were induced with IPTG. The protein was isolated from soluble fraction of the cell lysate through anion exchange chromatography. Finally, αA-crystallin fractions were purified further through a Sephacryl S300-HR exclusion size column and dialyzed against either 100 mM phosphate buffer or 50 mM Tris-HCl buffer (*p*H 7.4). All other chemicals including buffer salts were obtained from Sisco Research Laboratories (India) and were of analytical grade.

C. Protein labeling

There are two cysteine residues in αA-crystallin, cys131 and cys142. Of these, cys131 is much more reactive and is predominantly modified (Scheme 2(c)).[20] cys131 of the αA-crystallin domain was site selectively labeled with acrylodan and 1,5-IAEDANS. For fluorescent labeling, required quantity of a concentrated stock solution (~100 mM) of the probe in dimethylformamide (DMF) was added to a 30 μM αA-crystallin solution in 100 mM phosphate buffer (*p*H 7.4) containing 150 mM NaCl such that finally the protein and the probe had a molar ratio of ~1:5. The solution was incubated for four hours in the dark with constant stirring, followed by termination of the reaction with β-Mercaptoethanol (final concentration ~10 mM). The mixture was extensively dialyzed against ~4.5 L of 50 mM Tris-HCl buffer (*p*H 7.4) for two days with five changes. The labeling efficiency was spectrophotometrically assessed considering a molar extinction coefficient (ε) of 16 000 M^{-1} cm^{-1} at 280 nm for αA-crystallin and 19 000 M^{-1} cm^{-1} at 391 nm, and 5700 M^{-1} cm^{-1} at 336 nm for acrylodan and 1,5-IAEDANS, respectively. Necessary corrections were performed to negate the contribution

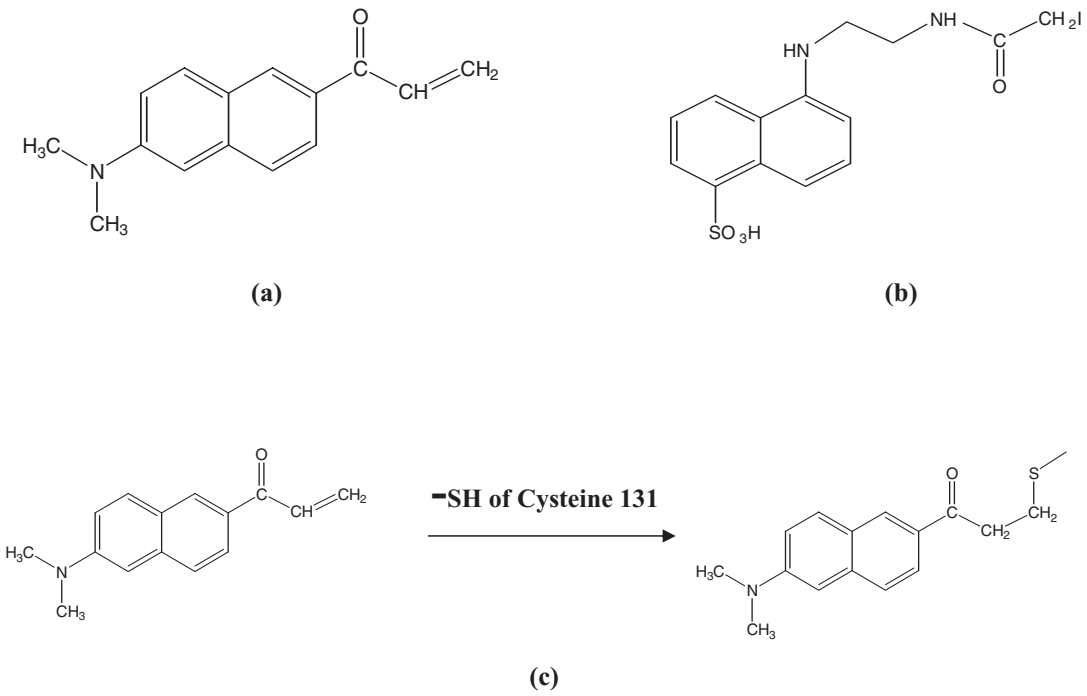

SCHEME 2. (a) Acrylodan (6-acrylolyl-2-dimethylaminonaphtalene). (b) 1,5-IAEDANS [5-((((2-iodoacetyl)amino)ethyl)amino) naphthalene-1-sulfonic acid]. (c) Protein labeling reaction scheme.

of the probes in absorbance at 280 nm. The labeling efficiency was found to be ∼50% for acrylodan and ∼65% for 1,5-IAEDANS. Absorption was recorded in Shimadzu UV-2400 spectrophotometer.

D. Circular dichroism (CD) spectropolarimetry

Protein samples (5 μM) were prepared both at native condition and in presence of 1 wt. % NaDC (in 50 mM Tris-HCl, *p*H 7.4). Far UV CD spectra were recorded on a Jasco J-720 spectropolarimeter by scanning from 200 nm to 260 nm using 1 mm path length cuvette. Protein-only spectra were obtained by subtracting the CD signal from that for the corresponding buffer. Five scans were taken for each sample with a step size of 0.5 nm and 5 s averaging time.

E. Steady state fluorescence

All steady state measurements were made in Hitachi F-7000 spectroflourimeter. The quenching data were analyzed in terms of the Stern-Volmer equations

$$\frac{\mathrm{I}_0}{\mathrm{I}} = 1 + \tau_0 k_q[\mathrm{Q}] = 1 + \mathrm{K_D}[\mathrm{Q}], \tag{1}$$

$$\frac{\tau_0}{\tau} = 1 + \tau_0 \mathrm{k_q}[\mathrm{Q}], \tag{2}$$

where ratio I_0/I is the intensity ratio and τ_0/τ is the lifetime ratio (I_0 and τ_0 being intensity and lifetime in absence of quencher), $\mathrm{K_D}$ is the dynamic quenching constant, $\mathrm{k_q}$ is the bimolecular quenching rate constant, and [Q] is the molar concentration of the quencher.

F. Time resolved studies

Our femtosecond up-conversion setup (FOG 100, CDP) is described in our earlier works.[48] To fit the femtosecond data one needs to know the long decay components. They were detected from a picosecond setup also described in our earlier works.[48] All experiments were done at room temperature (298 K).

The time resolved emission spectra (TRES) were constructed using the parameters of best fit to the fluorescence decays and the steady state emission spectrum following the procedure described by Maroncelli and Fleming.[49] Both the solvation dynamics (construction of solvent correlation function C(t)) and the fluorescence anisotropy decay was studied following our earlier procedure.[48]

The amount of solvation missed is calculated using the Fee-Maroncelli procedure.[50] The emission frequency at time zero, $\nu^p_{em}(0)$, may be calculated using the absorption frequency (ν^p_{abs}) in a polar medium (i.e., probe bound to αA-crystallin) as

$$\nu^p_{\mathrm{em}}(0) = \nu^p_{\mathrm{abs}} - \left(\nu^{np}_{\mathrm{abs}} - \nu^{np}_{\mathrm{em}}\right), \tag{3}$$

where ν^{np}_{em} and ν^{np}_{abs} denote the steady-state frequencies of emission and absorption, respectively, of the probe in a nonpolar solvent. After binding to the protein, acrylodan resembles 6-propionyl-2-(N,N-dimethylamino)-naphthalene (PRODAN). Thus, we used absorption and emission maxima of PRODAN in n-heptane as the nonpolar solvent.

All ensemble spectroscopic measurements were made with 20 μM protein and in 50 mM Tris-HCl buffer (*p*H-7.4). Thus the concentration of the dye labeled protein varied from 10 to 13 μM.

G. Microscopy

The protein samples were studied by FCS using a confocal microscope (PicoQuant, MicroTime 200) with an inverted optical microscope (Olympus IX-71). The details of the instrument have been described in our earlier works.[51] In brief, a water immersion objective (60X, 1.2 NA) was used to focus the excitation light 405 nm from a pulsed diode laser (PDL 828-S "SEPIA II," PicoQuant) on to the sample placed on a coverslip. After collecting the fluorescence along the same path, it was allowed to pass through a dichroic mirror and appropriate bandpass filters. We used a filter (HQ430lp) to block the exciting light. To detect the fluorescence a suitable bandpass filter (HQ480/40 m) was used. The fluorescence was then focused through a pinhole (50 μm) onto a beam splitter prior to entering two single-photon counting avalanche photodiodes (SPADs). The fluorescence autocorrelation traces were recorded by using two detectors (SPADs). The signal was subsequently processed by the PicoHarp-300 time-correlated single photon counting card (PicoQuant) to generate the autocorrelation function, $G(\tau)$. During the FCS experiments the laser power was kept at ~65 μW.

Data analysis of individual correlation curve was performed using the SymPhoTime software supplied by PicoQuant. The correlation function $G(\tau)$ of the fluorescence intensities is given by[52]

$$G(\tau) = \frac{\langle \delta F(0) \delta F(\tau) \rangle}{\langle F \rangle^2}, \tag{4}$$

where, $\langle F \rangle$ is the average intensity and $\delta F(\tau)$ is the fluctuations in intensity at a delay τ around the mean value, i.e., $\delta F(\tau) = \langle F \rangle - F(\tau)$.

In order to fit the correlation functions, we used 3D diffusion model having a triplet contribution (SymPho Time). For K fractions of dye diffusing within a system with distinct diffusion constants, the correlation function $G(\tau)$ is given by[52]

$$G(\tau) = \frac{1 - T + T\exp(-\tau/\tau_{tr})}{N(1-T)} \times \sum_{i=1}^{K} \phi_i \left(1 + \tau/\tau_i\right)^{-1} \left(1 + \tau/\tau_i S^2\right)^{-1/2}. \tag{5}$$

In the above equation, τ_i denotes the average time a dye molecule resides in the confocal volume, τ_{tr} is the life time of a dye molecule in its triplet state, τ is the delay or the lag time, N is the average number of molecules in the excitation volume, and T indicates the fraction of molecule in triplet state. S ($=w_z/w_{xy}$) is the structure parameter of the excitation volume, w_z and w_{xy} are the longitudinal and transverse radii, respectively. Structure parameter (S) of the excitation volume was calibrated using a sample (R6G in water) of known diffusion constant ($D_t = 426\ \mu m^2/s$).[53] The estimated volume of the excitation volume is ~ 0.75 fL with a transverse radius (w_{xy}) ~ 305 nm. All the FCS and microscopy measurement were done at 293 K. Diffusion constant (D_t) was calculated from the following equation:

$$\tau_i = \frac{w_{xy}^2}{4D_t}, \tag{6}$$

From the calculated value of diffusion constant (D_t) one can easily determine the hydrodynamic radius (r_h) of the diffusing species using the Stokes-Einstein equation

$$r_h = \frac{k_B T}{6\pi \eta_0 D_t}. \tag{7}$$

As the diffusion coefficient varies inversely with viscosity, the viscosity of 1 wt. % NaDC at room temperature was evaluated from flow rate measurements in a homemade Ostwalds viscometer.

III. RESULTS AND DISCUSSIONS

During all the FCS measurements the protein concentration kept fixed at ~2 nM such that the dye labeled protein concentration remains ~1 nM (in 50 mM Tris-HCl buffer, *p*H 7.4). All the bulk (ensemble) studies for steady state, picosecond and femtosecond up-conversion techniques were done using ~20 μM protein solution and in 50 mM Tris-HCl buffer (*p*H – 7.4). The CD experiment was done using ~5 μM protein solution in 50 mM Tris-HCl buffer (*p*H-7.4).

A. Fluorescence correlation spectroscopy and size of αA-crystallin tetramer in presence of NaDC

The size of the protein (αA-crystallin) in the absence and presence of NaDC was determined using FCS technique under a confocal microscope. Figure 1 shows the normalized autocorrelation curves of acrylodan covalently attached to αA-crystallin in the absence and presence of NaDC, while the actual autocorrelation curves are shown in the inset.

From the normalized autocorrelation curves it is clear that the diffusion of acrylodan covalently attached to αA-crystallin is much more slower compared to that of the same protein solution in presence of NaDC. The diffusion coefficient (D_t) of acrylodan-αA-crystallin system is found to be ~35 $\mu m^2\ s^{-1}$ in the absence of NaDC. This is ~2-fold smaller

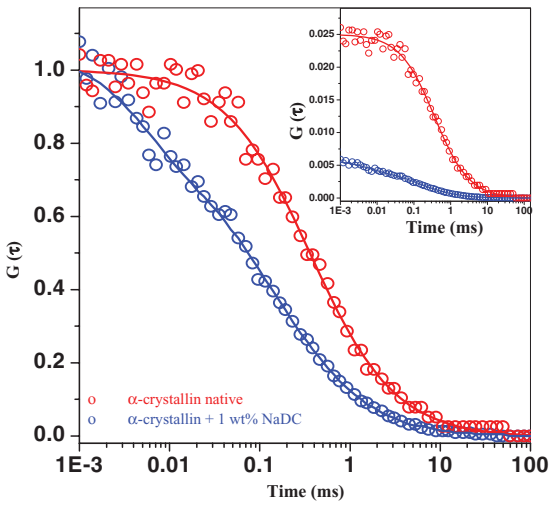

FIG. 1. Normalized auto-correlation functions of acrylodan-αA-crystallin system in the absence (red) and presence (blue) of 1 wt. % NaDC. Actual autocorrelation curves are shown in the inset.

(i.e., slower diffusion) compared to that of acrylodan-αA-crystallin system in the presence of NaDC ($D_t \sim 68\ \mu m^2\ s^{-1}$) (Figure 1). The faster diffusion signifies the formation of smaller fragments of the αA-crystallin oligomer upon addition of NaDC.

The viscosities of the solutions are found to be 0.89 cP and 0.97 cP, respectively, for the protein solution in the absence and presence of NaDC at room temperature. Using Eq. (7), the hydrodynamic radius (r_h) of the acrylodan-αA-crystallin system in the absence and presence of NaDC is calculated and found to be $\sim 6.9 \pm 0.1$ nm and $\sim 3.3 \pm 0.1$ nm, respectively. Thus addition of NaDC causes a 6.9/3.3 $\sim 2.1 \pm 0.1$ fold decrease in the hydrodynamic radius (r_h).

From the inset of Figure 1 it is readily seen that the magnitude of G(0) decreases nearly 5-fold when NaDC is added to αA-crystallin. Since about 50% of the proteins are labeled by acrylodan, the 5-fold decrease in G(0) corresponds to a 10-fold increase in number of particles within the confocal volume (N) as G(0) is inverselely proportional to N. It may be recalled that according to gel filtration studies of αA-crystallin, addition of NaDC causes a 10-fold reduction of molecular mass from ~800 kDa to ~80 kDa.[8,29] Molecular mass is roughly proportional to molecular volume and hence, proportional to cube of the hydrodynamic radius (r_h). Thus a 10-fold reduction in molecular mass is expected to result in a cube root of 10, i.e., 2.15 times reduction in the hydrodynamic radius (r_h). This is remarkably close to the 2.1 ± 0.1 fold decrease experimentally observed using FCS. This is also consistent with the 10-fold increase in number of particles as obtained from the decrease in G(0) (inset of Figure 1).

Thus, FCS results demonstrate that addition of NaDC to the αA-crystallin oligomer of mass ~800 kDa causes a 10-fold reduction in mass to ~80 kDa, i.e., to a tetramer of αA-crystallin. NaDC disrupts the inter-subunit contacts in higher oligomers forming tetrameric units of the protein. It is suggested that the N-terminal region of αA-crystallin is primarily involved in inter-subunit contacts in the oligomer.[5,54] In Sec. III B, we will show from steady state emission spectra and quenching studies that NaDC, indeed, makes the N-terminal region (and trp-9) more exposed.

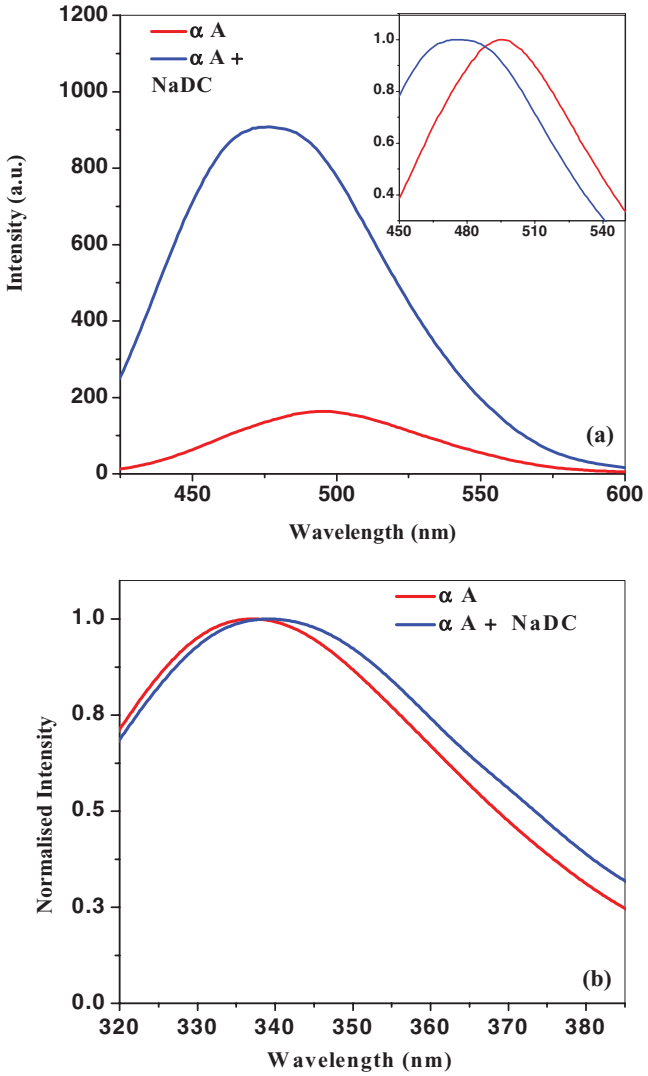

FIG. 2. (a) Emission spectra (at $\lambda_{ex} = 405$ nm) of acrylodan labeled αA-crystallin (~10 μM labeled protein in 50 mM Tris-HCl, *p*H-7.4) in native state (red) and in presence of NaDC (blue). The inset represents intensity normalized emission. (b) Normalized tryptophan emission spectra (at $\lambda_{ex} = 295$ nm) of αA-crystallin in native state (red) and in presence of NaDC (blue). The protein (20 μM) was in 50 mM Tris-HCl, *p*H-7.4.

B. Steady state emission: Effect of binding of NaDC to αA-crystallin

Acrylodan, bound to a protein (Scheme 1(b)) is a very good marker of the microenvironment polarity.[55–57] Acrylodan bound to αA-crystallin exhibits emission maximum (λ_{em}^{max}) ~495 nm. On addition of NaDC, λ_{em}^{max} displays a marked blueshift by 17 nm to 478 nm and shows an ~5-fold increase in quantum yield. Such a drastic blueshift and intensity increase indicates a lot more hydrophobic environment around the probe in presence of NaDC (Figure 2(a)) and suggests that NaDC binds to the protein near the acrylodan attached to cys-131.

In contrast to acrylodan, on addition of NaDC the intrinsic probe tryptophan exhibits a redshift in emission maximum from 337 nm to 339 nm suggesting a slightly more exposed tryptophan in tetrameric form (Figure 2(b)).

Acrylamide quenching provides further support to the contention that addition of NaDC makes the tryptophan residue (trp-9) more exposed while it creates a more hydrophobic environment around cys-131. For studying acrylamide quenching cys-131 is labeled by 1,5-IAEDANS (Scheme 2(b)). The Stern-Volmer plots of tryptophan quenching shows an increase in the k_q value from $\sim 1 \times 10^9\ M^{-1}\ s^{-1}$ in native to $\sim 2.2 \times 10^9\ M^{-1}\ s^{-1}$ in presence of 1 wt. % NaDC (Figure 3(a)) and hence increased solvent accessibility, indicating structural perturbations. The tryptophan Stern-Volmer plots showed linearity without any upward curvature arising from an apparent static quenching component and hence, they were analyzed without consideration of a sphere of action[38] for the quencher. Interestingly, quenching plots of 1,5-IAEDANS conjugated to cys-131 shows ~6-fold reduced quenching rate constant in presence of NaDC (Figure 3(b)). There was a decrease in the value of k_q from $2.1 \times 10^8\ M^{-1}\ s^{-1}$ to $0.36 \times 10^8\ M^{-1}\ s^{-1}$. Such marked decrease may be

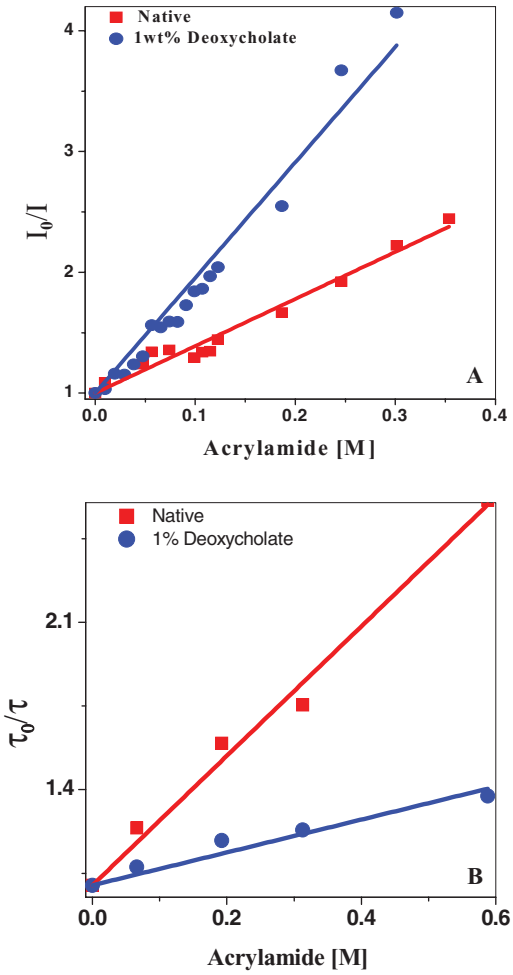

FIG. 3. (a) Stern-Volmer plot (at $\lambda_{ex} = 295$ nm) showing quenching of Trp 9 of αA-crystallin by acrylamide in native α A crystalline (red) and in presence of 1 wt. % NaDC (blue). The protein (20 μM) was in 50 mM Tris-HCl, *p*H-7.4. Figure represents average of three experiments. (b) Stern-Volmer plot (at $\lambda_{ex} = 340$ nm) showing quenching of 1,5-IAEDANS by acrylamide in native αA-crystallin (red) and in presence of 1 wt. % NaDC (blue). The protein (~13 μM labeled protein) was in 50 mM Tris-HCl, *p*H-7.4.

explained by considering the probe to be in a buried environment through interaction with NaDC aggregates. The linearity of the Stern-Volmer plot of 1,5-IAEDANS and its monoexponential lifetime is a signature of presence of single species[52] and thus reconfirmed the site selectivity of the labeling.

In summary, on addition of NaDC the tryptophan residue (trp-9) which is located near the N-terminal end of the chaperone αA-crystallin becomes more exposed to solvent (water), while the thiol region (cys-131) moves away from the solvent. Therefore, NaDC induces region specific conformational alteration in αA-crystallin exposing the terminal groups (trp-9) and shielding the region around cys-131 (labeled with acrylodan). The binding of NaDC near cys-131 is perhaps also the root cause of oligomeric breakdown as well as exposure of the terminal domains.

C. Circular dichroism

The CD spectra of the native form of αA-crystallin oligomer (~800 kDa) exhibits a minima (Figure 4) around

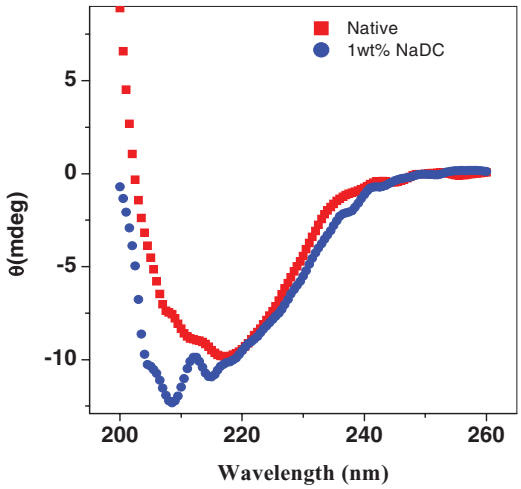

FIG. 4. Far-UV CD spectra of αA-crystallin (5 μM) in the absence (red) and in the presence of 1 wt. % NaDC (blue).

217 nm as reported previously.[29,58,59] This is characteristics of predominant β-sheet structure of αA-crystallin.[29,58,59] In the presence of 1 wt. % NaDC there is a shift in position of the minima and a new minima was detected below 210 nm without significant lowering of the ellipticity values. This indicates a possible increase in random-coil conformation due to tetramerization.[57,58] This is qualitatively consistent with the CD spectra previously reported by Kantorow *et al.*[29] In summary, NaDC causes a slight increase in the contribution of random coil conformation without drastically perturbing the secondary structure of αA-crystallin. In contrast 1% sodium dodecyl sulphate (SDS) extensively alters the structure of αA-crystallin oligomer.[29,30]

D. Picosecond and femtosecond solvation dynamics

In this section, we show that binding of NaDC affect solvation dynamics of acrylodan bound to cys-131 of αA-crystallin. This is very similar to the slowing down of the solvation dynamics at the active site of the enzyme on binding of a substrate, reported earlier.[34]

The picosecond and femtosecond transients of acrylodan in acrylodan-αA-crystallin complex both in the absence and presence of NaDC are shown in Figures 5 and 6. The picosecond and femtosecond transients of both the systems depend on emission wavelength. For both the systems, at the red end (long emission wavelength) a rise precedes the decay. No such rise is observed at the blue end. The rise at the red end and decay at the blue end is a clear signature of solvation dynamics.

The femtosecond transient of the acrylodan-αA-crystallin system exhibits three decay components (1, 36, and 2200 ps) at the blue end ($\lambda_{em} = 470$ nm) (Figure 6). However, at the red end ($\lambda_{em} = 540$ nm) a rise component (1.5 ps) precedes the two long decay components (480 and 3300 ps). Upon addition of NaDC to the native acrylodan-αA-crystallin oligomeric system, the decay components at the blue end become 3, 35, and 3000 ps. At the red end, there is one rise component (4 ps) and two long decay components (260 and 4160 ps) (Figure 6). The increase in rise time (from 1.5 ps in

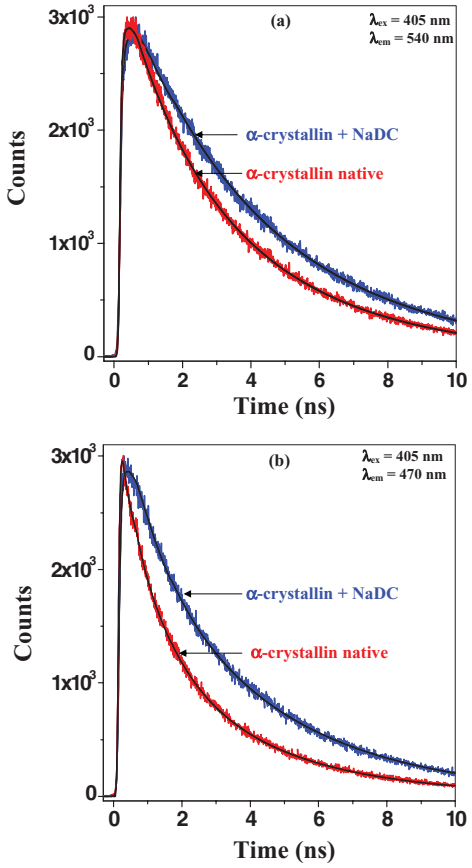

FIG. 5. Picosecond transients of acrylodan -αA-crystallin system (at λ_{ex} = 405 nm) in the absence (red) and presence (blue) of NaDC at (A) λ_{em} = 540 nm and (B) λ_{em} = 470 nm.

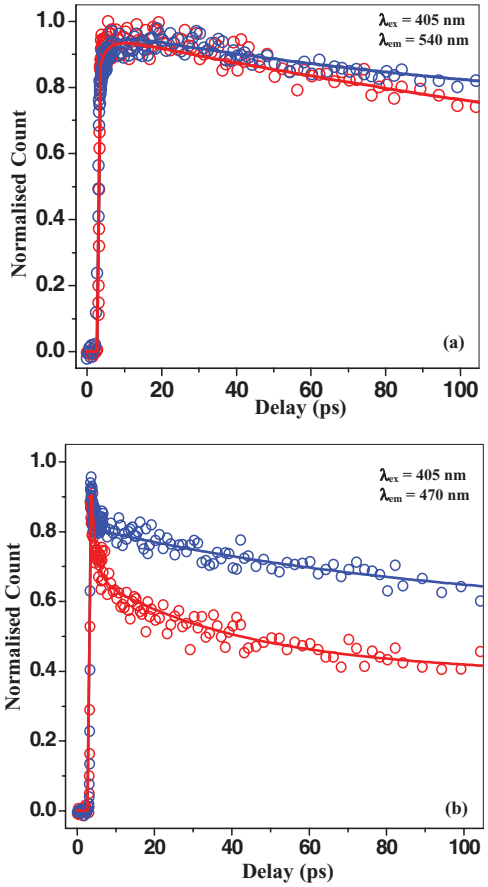

FIG. 6. Femtosecond transients of acrylodan -αA-crystallin system (at λ_{ex} = 405 nm) in the absence (red) and presence (blue) of NaDC at (A) λ_{em} = 540 nm and (B) λ_{em} = 470 nm.

the absence of NaDC to 4 ps in the presence of NaDC) at the red end indicates a slower solvent relaxation in presence of NaDC.

Figure 7 shows the TRES of acrylodan-αA-crystallin system in the presence and absence of NaDC. The total dynamic Stokes shift, $\Delta\nu = \nu(0) - \nu(\infty)$ in acrylodan-αA-crystallin and acrylodan-αA-crystallin/NaDC systems were observed to be 1100 and 1200 cm^{-1}, respectively (Table I). Table I further shows that the $\nu(0)$ in the presence of NaDC (22 100 cm^{-1}) is blueshifted from that in the absence of NaDC (21 300 cm^{-1}) by about 800 cm^{-1}. This suggests a less polar environment in the presence of NaDC and is consistent with the observed blueshift of the steady state emission maximum. This suggests that NaDC makes the micro-environment around cys-131 more hydrophobic and hence more buried.

Figure 8 shows the decay of solvent correlation function, C(t), and the decay parameters were summarized in Table I. From Table I it is observed that the average solvation time of acrylodan-αA-crystallin system is ~240 ps, this is ~2-fold faster compared to that of acrylodan-αA-crystallin in presence of NaDC (~520 ps). Thus binding of NaDC to the protein near cys-131 makes the motion of the confined water molecules more restricted and thus solvation dynamics becomes slower.

The ultrafast components of solvation (1 ps and 2.5 ps components for acrylodan-αA-crystallin system in the absence and presence of NaDC) may arise due to the dielectric relaxation or librational motion of the free water molecules.[34–46] The slow components of solvation of acrylodan bound to αA-crystallin (25 ps and 800 ps in the absence and 30 ps and 800 ps in the presence of NaDC) may be assigned to the motion of the hydrogen bonded water molecules residing at the hydration layer as well as other electrostatic interaction in the oligomeric protein.[40,41] As noted in many recent simulations, such interaction leads to the formation of an hydrogen bond network around a protein which is stabilized by quasi-stable hydrogen bonds ("pinning sites").[42–46] The hydrogen bond network and bound-to-free inter-conversion[41] gives rise to an anomalously slow dynamics of the structured and quasi-bound water molecules ("biological water") around a protein. The 25–30 ps component may be ascribed to bound water. The longer component in 800 ps may arise from Rouse chain dynamics of polymer chain dynamics.[34,36]

In summary, the solvation dynamics further corroborates that NaDC binds near the cys-131 group and makes the local environment more restricted. The 2-fold slowing down of solvation dynamics of acrylodan and the 800 cm^{-1} blueshift in $\nu(0)$ gives further support to the contention that NaDC binds near cys-131 of αA-crystallin.

Finally, we comment on how binding of NaDC near cys-131 affect enhanced auto-phosphorylation of αA-crystallin. We have already discussed several possible sites of phosphorylation in αA-crystallin. NaDC binds near the cys-131 region

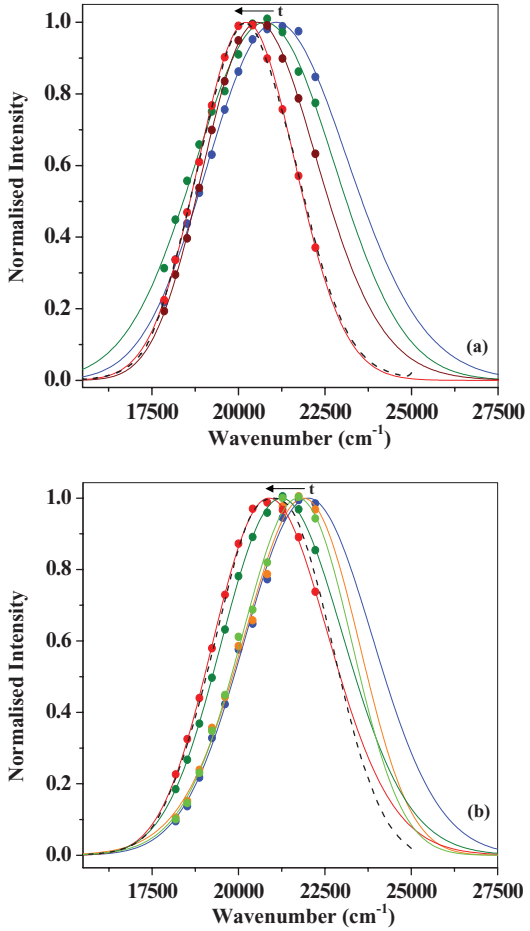

FIG. 7. Time-resolved emission spectra (TRES) of acrylodan -αA-crystallin system (λ_{ex} = 405 nm) (a) in the absence of NaDC at 0 ps (blue), 20 ps (olive), 200 ps (wine red), and 3500 ps (red) (b) in the presence of NaDC at 0 ps (blue), 10 ps (orange), 40 ps (green), 800 ps (olive), and 3500 ps (red). The steady state emission spectra were shown in the black dotted line.

that acts as a hinge region connecting the terminal domains with the central αA-crystallin domain. Blockage of this region by NaDC binding possibly leads to shielding of all the nearby phosphorylation sites, e.g., ser-127, 130, 132, and 134 including ser-122 and thr-140. Since, the terminal regions of αA-crystallin become exposed due to binding of NaDC near cys-131, enhanced phosphorylation takes place at the sites located in the terminal regions. Thus the possible sites of phosphorylation at N-terminal region may be thr-13 (near trp-9)

TABLE I. Decay parameters of C(t) of acrylodan-αA-crystallin system in the absence and presence of NaDC.

System	$\Delta\nu$ [$\nu(0)$] cm^{-1}	τ_1 [ps] (a_1)	τ_2 [ps] (a_2)	τ_3 [ps] (a_3)	τ_4 [ps] (a_4)	$\langle\tau\rangle$ [ps]
α-A-crystallin	1100 [21 300]	≤ 0.3[a] (0.5)	1 (0.10)	25 (0.10)	800 (0.30)	240
α-A-crystallin + 1 wt. % NaDC	1200 [22 100]	≤ 0.3[a] (0.2)	2.5 (0.04)	30 (0.12)	800 (0.64)	520

[a]Calculated using Fee-Maroncelli method (Ref. 50).

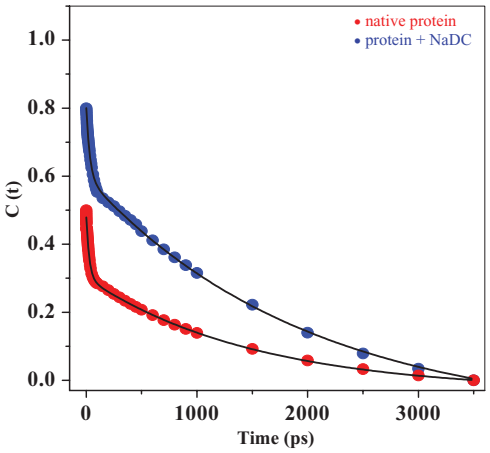

FIG. 8. Decay of the solvent response function, C(t) of αA-crystallin system in the absence (red) and presence (blue) of NaDC. The points denote the actual values of C(t) and the solid line denotes the best fit.

or ser-45 position (Schemes 3(a) and 3(b)). At the C-terminal region of the 173 amino acids of αA-crystallin the possible phosphorylation sites are serines 169 and 172. The increased activity of the C-terminal and N-terminal serines and threonine is further supported by the fact that NaDC makes the trp-9 near the N-terminal more exposed.

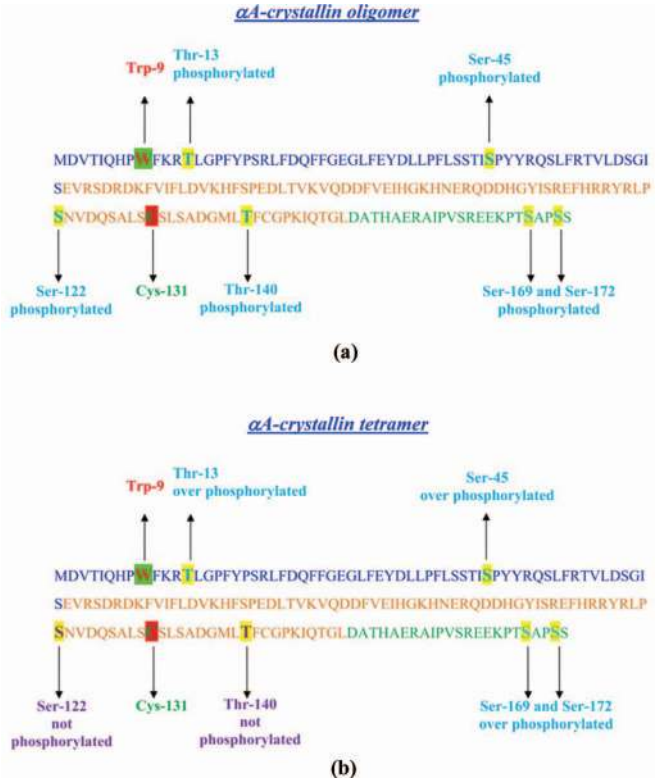

SCHEME 3. Schematic representation of amino acid sequence and possible phosphorylation sites of human αA-crystallin subunit (a) in oligomeric form (in absence of NaDC) and (b) in tetrameric form (in presence of NaDC). 1-62 amino acid residues represent N-terminal region (blue), while 63-150 residues represent "central α-crystallin domain" (orange) and 151-173 residues exhibit the C-terminal tail (green).[54]

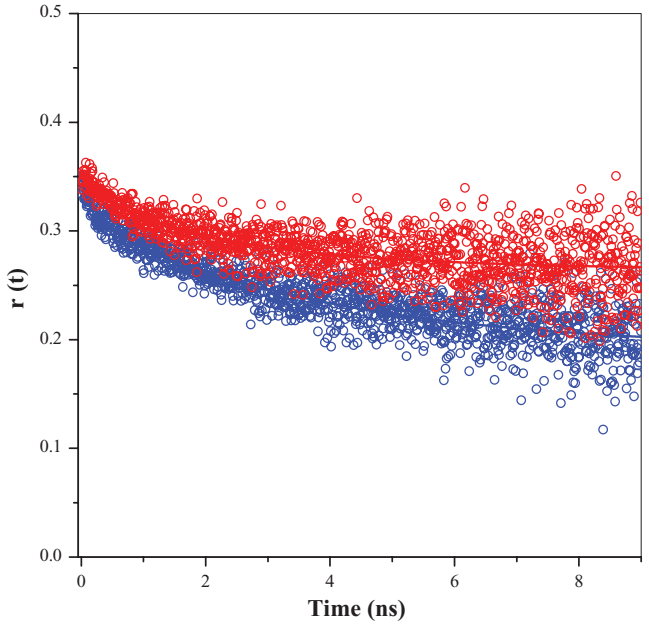

FIG. 9. Fluorescence anisotropy decay of acrylodan -αA-crystallin system (at $\lambda_{ex} = 405$ nm) along with a fitted curve in the absence (red) and presence (blue) of NaDC at $\lambda_{em} = 480$ nm.

E. Fluorescence anisotropy decay

The fluorescence anisotropy decays of acrylodan bound to αA-crystallin both in the presence and absence of NaDC was fitted to a bi-exponential decay (Figure 9). The decay parameters are summarized in Table II. Acrylodan-αA-crystallin system displays a relatively fast component of ~1.1 ns and slow component of ~14 ns. In the presence of NaDC a fast component of ~1.4 ns and a slow component of ~8 ns is obtained.

The lifetime of the covalent probe acrylodan is too short (~4 ns) to faithfully report the long component of anisotropy decay in 10 ns time scale. The high value of anisotropy at t = 0 (time zero) suggests that most of the rotational relaxation dynamics is captured in our picosecond setup. The very slow component (~10 ns) of anisotropy decay may be attributed to the overall tumbling motions of the monomer subunit and not the oligomers since oligomeric αA-crystallin (r_h ~6.9 nm) would have an enormously long correlation time (on the order of 100 ns), which can never be detected with a probe whose excited state lifetime is 4 ns.

The ~1.8-fold decrease of the long component (from 14 ns in the absence of NaDC to 8 ns in the presence of NaDC) in case of the tetramer may be due to the subunits having larger extent of freedom for tumbling motion or due to increased compactness of the subunits in the tetramer. The rapid exchange of αA-crystallin subunits may be responsible for the tumbling motion of individual subunits independent of the overall motion of the oligomer.[20]

TABLE II. Anisotropy decay of acrylodan-αA-crystallin system in the absence and presence of NaDC.

System	r_0	τ_{r1} [ns] (a_1)	τ_{r2} [ns] (a_2)	$\langle\tau_r\rangle$ [ns]
α-A-crystallin	0.35	1.1 (0.48)	14.0 (0.52)	7.8
α-A-crystallin + 1 wt. % NaDC	0.35	1.4 (0.21)	8.0 (0.69)	5.8

The relatively faster component (~1 ns = 1000 ps) may be assigned to the segmental chain motion of the protein or the local motion of the probe molecule. With the addition of NaDC the fast component slightly increases from 1.1 ns (1100 ps) to 1.4 ns (1400 ps). This indicates that NaDC restricts the segmental chain motion or local motion of the probe molecule by binding to the protein near the probe molecule.

IV. CONCLUSION

In this work using FCS we demonstrate that addition of NaDC leads to disintegration of the αA-crystallin oligomer into tetramer. The substantial blueshift and slower solvation dynamics on addition of the NaDC indicates that NaDC bind near the cys-131 (labeled by acrylodan) of αA-crystallin tetramer. It is shown that binding of NaDC causes region dependent conformation change. The 17 nm blueshift of acrylodan, 2-fold retardation of solvation dynamics, and 800 cm^{-1} blueshift of $\nu(0)$ suggests that NaDC binds near cys-131 and makes this region more shielded and restricted. The redshift of trp-9 emission and the increased quenching suggests that NaDC makes the terminal region more exposed. This result may reinforce the idea that increased auto-phosphorylation activity of αA-crystallin tetramer formed in the presence of NaDC may involve the C-terminal serines (169 and 172) and N-terminal threonine (13) and serine (45) and does not involve ser-122.

ACKNOWLEDGMENTS

We would like to thank Dr. W. W. de Jong of Katholic University, The Netherlands, for the gift of plasmid DNA for αA-crystallin. We are also grateful to Professor S. Basak (SINP, Kolkata, India) for allowing us to use the 295 nm and 340 nm excitation sources and for several helpful discussions and insights. Thanks are due to Department of Science and Technology, India (Center for Ultrafast Spectroscopy and Microscopy, J. C. Bose Fellowship), and the Council of Scientific and Industrial Research (CSIR) for generous research grants. S.S.M. and D.K.S. thank CSIR for awarding fellowships. We also acknowledge the constructive comments of the reviewers.

[1] J. Forrester, A. Dick, P. McMenamin, and W. Lee, *The Eye: Basic Sciences in Practice* (W. B. Saunders Company Ltd., London, 1996), p. 28.
[2] J. Harding, *Cataract: Biochemistry, Epidemiology and Pharmacology* (Chapman and Hall, London, 1991).
[3] H. J. Hoenders and H. Bloemendal, *Molecular and Cellular Biology of the Eye Lens*, edited by H. Bloemendal (Wiley, New York, 1981), p. 279.
[4] W. W. De Jong, *Evolution of Lens Crystallins. In Molecular and Cellular Biology of the Eye Lens*, edited by H. Bloemendal (Wiley-Interscience, New York, 1981), p. 221.
[5] F. Narberhaus, Microbiol. Mol. Biol. Rev. **66**, 64 (2002).
[6] W. W. de Jong, E. C. Terwindt, and H. Bloemendal, FEBS Lett. **58**, 310 (1975).
[7] F. J. Van der Ouderaa, W. W. de Jong, and H. Bloemendal, Eur. J. Biochem. **39**, 207 (1973).
[8] J. Horwitz, Exp. Eye Res. **88**, 190 (2009).
[9] J. Horwitz, Proc. Natl. Acad. Sci. U.S.A. **89**, 10449 (1992).

[10]K. P. Das and W. K. Surewicz, Biochem. J. **311**, 367 (1995).
[11]K. P. Das, J. M. Petrash, and W. K. Surewicz, J. Biol. Chem. **271**, 10449 (1996).
[12]K. P. Das and W. K. Surewicz, FEBS Lett. **369**, 321 (1995).
[13]B. Raman and C. M. Rao, J. Biol. Chem. **269**, 27264 (1994).
[14]P. V. Rao, J. Horwitz, and J. S. Zigler, Biochem. Biophys. Res. Commun. **190**, 786 (1993).
[15]K. Wang and A. Spector, J. Biol. Chem. **269**, 13601 (1994).
[16]Z. T. Farahbakhsh, Q. L. Huang, L. L. Ding, C. Altenbach, H. J. Steinhoff, J. Horwitz, and W. L. Hubbell, Biochemistry **34**, 509 (1995).
[17]D. A. Haley, J. Horwitz, and P. L. Stewart, J. Mol. Biol. **277**, 27 (1998).
[18]D. A. Haley, M. P. Bova, Q. L. Huang, H. S. Mchaourab, and P. L. Stewart, J. Mol. Biol. **298**, 261 (2000).
[19]S. Saha and K. P. Das, Proteins **57**, 610 (2004).
[20]M. P. Bova, L. L. Ding, J. Horwitz, and B. K. Fung, J. Biol. Chem. **272**, 29511 (1997).
[21]T. X. Sun, N. J. Akhtar, and J. J. Liang, FEBS Lett. **430**, 401 (1998).
[22]R. J. Siezen, J. G. Bindels, and H. J. Hoenders, Eur. J. Biochem. **107**, 243 (1980).
[23]M. T. Walsh, A. C. Sen, and B. Chakrabarti, J. Biol. Chem. **266**, 20079 (1991).
[24]G. Wistow, Exp. Eye Res. **56**, 729 (1993).
[25]R. H. Smulders, M. A. van Boekel, and W. W. de Jong, Int. J. Biol. Marcomol. **22**, 187 (1998).
[26]I. K. Feil, M. Malfois, J. Hendle, H. van Der Zandt, and D. I. Svergun, J. Biol. Chem. **276**, 12024 (2001).
[27]K. B. Merck, P. J. T. A. Groenen, C. E. M. Voorter, W. A. de Haard-Hoekman, J. Horwitz, H. Bloemendal, and W. W. de Jong, J. Biol. Chem. **268**, 1046 (1993).
[28]S. Jehle, P. Rajagopal, B. Bardiaux, S. Markovic, R. Kühne, J. R. Stout, V. A. Higman, R. E. Klevit, B. J. van Rossum, and H. Oschkinat, Nat. Struct. Biol. **17**, 1037 (2010).
[29]M. Kantorow, J. Horwitz, M. A. M. van Boekel, W. W. de Jong, and J. Piatigorsky, J. Biol. Chem. **270**, 17215 (1995).
[30]A. Biswas and K. P. Das, Protein J. **23**, 529 (2004).
[31]T. Aerts, J. Clauwaert, P. Haezebrouck, E. Peeters, and H. Van Dael, Eur. Biophys. J. **25**, 445 (1997).
[32]L. J. Takemoto Exp. Eye Res. **62**, 499 (1996).
[33]M. J. MacCoss, W. H. McDonald, A. Saraf, R. Sadygov, J. M. Clark, J. J. Tasto, K. L. Gould, D. Wolters, M. Washburn, A. Weiss, J. I. Clark, and J. R. Yates, Proc. Natl. Acad. Sci. U.S.A. **99**, 7900 (2002).
[34]S. Guha, K. Sahu, D. Roy, S. K. Mondal, S. Roy, and K. Bhattacharyya, Biochemistry **44**, 8940 (2005).
[35]D. Mandal, S. Sen, D. Sukul, K. Bhattacharyya, A. K. Mandal, R. Banerjee, and S. Roy, J. Phys. Chem. B **106**, 10741 (2002).
[36]S. K. Pal, J. Peon, B. Bagchi, and A. H. Zewail, J. Phys. Chem. B **106**, 12376 (2002).
[37]D. P. Zhong, S. K. Pal, and A. H. Zewail, Chem. Phys. Lett. **503**, 1 (2011).
[38]A. Jha, K. Ishii, J. B. Udgaonkar, T. Tahara, and G. Krishnamoorthy, Biochemistry **50**, 397 (2011).
[39]K. Bhattacharyya, Chem. Commun. **2008**, 2848.
[40]N. Nandi, K. Bhattacharyya, and B. Bagchi, Chem. Rev. **100**, 2013 (2000).
[41]N. Nandi and B. Bagchi, J. Phys. Chem. A **102**, 8217 (1998).
[42]S. Bandyopadhyay, S. Chakraborty, S. Balasubramanian, and B. Bagchi, J. Am. Chem. Soc. **127**, 4071 (2005).
[43]S. Bandyopadhyay, S. Chakraborty, and B. Bagchi, J. Am. Chem. Soc. **127**, 16660 (2005).
[44]W. H. Thompson, J. Chem. Phys. **120**, 8125 (2004).
[45]K. R. Mitchell-Koch and W. H. Thompson, J. Phys. Chem. C **111**, 11991 (2007).
[46]F. Pizzitutti, M. Marchi, F. Sterpone, and P. J. Rossky, J. Phys. Chem. B **111**, 7584 (2007).
[47]A. Biswas and K. P. Das, J. Biol. Chem. **279**, 42648 (2004).
[48]D. K. Sasmal, S. Sen Mojumdar, A. Adhikari, and K. Bhattacharyya, J. Phys. Chem. B **114**, 4565 (2010).
[49]M. Maroncelli and G. R. Fleming, J. Chem. Phys. **86**, 6221 (1987).
[50]R. S. Fee and M. Maroncelli, Chem. Phys. **183**, 235 (1994).
[51]S. Ghosh, A. Adhikari, S. Sen Mojumdar, and K. Bhattacharyya, J. Phys. Chem. B **114**, 5736 (2010).
[52]J. R. Lakowicz, *Principles of Fluorescence Spectroscopy*, 3rd ed. (Springer, New York, 2006), Chaps. 8 and 24.
[53]Z. Petrasek and P. Schwille, Biophys. J. **94**, 1437 (2008).
[54]M. Kundu, P. C. Sen, and K. P. Das, Biopolymers **86**, 177 (2007).
[55]G. Weber and F. J. Farris, Biochemistry **18**, 3075 (1979).
[56]F. G. Prendergast, M. Meyer, G. L. Carlson, S. Iida, and J. D. Potter, J. Biol. Chem. **258**, 7541 (1983).
[57]B. C. Lobo and C. J. Abelt, J. Phys. Chem. A **107**, 10938 (2003).
[58]S. Mukhopadhyay, M. Kar, and K. P. Das, Protein J. **29**, 551 (2011).
[59]A. Biswas, A. Miller, T. Oya-Ito, P. Santhoshkumar, M. Bhat, and R. H. Nagaraj, Biochemistry **14**, 4569 (2006).
[60]A. Roy, A. Kucukural, and Y. Zhang, Nat. Protoc. **5**, 725 (2010).
[61]Y. Zhang, BMC Bioinf. **9**, 40 (2008).